# Electronic Supplementary Information for Intermetallic molybdenum disilicide: A new, active, and stable cocatalyst for efficient solar hydrogen production

Fang Wang,[a] Wenbo Li,[a] Hui Pan,[a] Zhengguo Zhang,[a] Chao Kong[b] and Shixiong Min*[a]

[a] *School of Chemistry and Chemical Engineering, North Minzu University, Yinchuan 750021, China. E-mail: sxmin@nun.edu.cn*

[b] *College of Chemistry and Chemical Engineering, Longdong University, Qingyang 745000, China.*

## 1. Experimental

### 1.1 Chemicals and reagents

$MoSi_2$ powder was purchased from HeFei KeRun Nanometer Technology Development Co., Ltd. $NiSi_2$, $WSi_2$, $VSi_2$, and $FeSi_2$ powders were purchased from Tansoole (China). $Mo_2B_5$ powder was purchased from Hefei ZhongHang Nanometer Technology Development Co., Ltd. Triethanolamine (TEOA, 99.8%) was purchased from Xilong Scientific Co., Ltd. Erythrosin B (ErB), Eosin Y (EY), Rose Bengal (RB), Fluorescein sodium (FS), and Rhodamine B were obtained from Tianjin Guangfu Fine Chemical Research Institute. Hydrofluoric acid solutoin (HF, 48~51%, Damas-beta) and sodium sulfate ($NaSO_4$, >99.5%) were purchased from Tansoole (China). $TiO_2$ nanoparticles (P25, 20% rutile and 80% anatase) were purchased from Degussa. Ammonium tetrathiomolybdate ($(NH_4)_2MoS_4$) and CdS nanoparticles were synthetized according to the reported methods.[S1,S2] All solutions were prepared using ultrapure water (18.2 MΩ cm).

### 1.2 Catalyst treatment and preparation

#### 1.2.1 Etching treatment of $MoSi_2$

1.0 g of commercial $MoSi_2$ powder was dispersed in 50 mL of 1 M HF solution and ultrasonicated for 30 min. After that, etching reaction was allowed to be proceeded for 6 h under stirring at room temperature. The obtained products were collected by centrifugation, washed three times with degassed water, and dried in vacuum at 60 °C for 12 h.

#### 1.2.2 Synthesis of $MoS_2$ catalyst

$MoS_2$ catalyst was synthesized by direct thermal decomposition of $(NH_4)_2MoS_4$ according to the previously reported method.[S3] Briefly, 300 mg of $(NH_4)_2MoS_4$ was directly annealed in an $N_2$ atmosphere at 800 °C for 5 h with a ramping rate of 5 °C $min^{-1}$. The obtained products were washed twice with water and ethanol, respectively, and dried in vacuum at 60 °C for 12 h.

#### 1.2.3 Synthesis of $CdS/MoSi_2$ and $TiO_2/MoSi_2$ composite photocatalysts

$CdS/MoSi_2$ (10 wt%) and $TiO_2/MoSi_2$ (10 wt%) composite photocatalysts were

synthesized by a facile solution-based mixing method. Briefly, 1.0 g of CdS or $TiO_2$ nanoparticles was dispersed into 200 mL of water containing 10 wt% $MoSi_2$ in ultrasonication. After 30 min stirring, the products were collected by filtration, and then dried in vacuum at 60 °C for 12 h.

**1.3 Materials characterizations**

X-ray diffraction (XRD) measurements were performed on a Rigaku Smartlab diffractometer using a nickel filtrated Cu *K*α radiation source at 40 kV and 40 mA. Scanning electron microscopy (SEM) images were taken with a ZEISS Sigma 500 scanning electron microscope. Transmission electron microscopy (TEM) and high-resolution TEM (HRTEM) images were taken with a Tecnai-$G^2$-F30 field emission transmission electron microscope. X-ray photoelectron spectroscopy (XPS) measurements were performed on a Thermo Scientific Escalab-250Xi electron spectrometer using a monochromatic Al *K*α X-ray source (1486.6 eV). The binding energies were referenced to the C 1s peak at 284.8 eV. UV-vis diffuse reflectance spectra were recorded on a PerkinElmer Lambda-750 UV-vis-near-IR spectrometer equipped with an integrating sphere and $BaSO_4$ powder was used as the reflectance standard. UV-vis absorption spectra were taken with a Thermo Scientific Evolution 220 spectrophotometer. Photoluminescence spectra were determined by a Horiba Scientific FluoroMax-4 spectrofluorometer spectrometer. The specific surface areas of the samples were determined by nitrogen adsorption-desorption isotherms using the Brunauer-Emmett-Teller (BET) method (Micromeritics ASAP 2460).

**1.4 Photocatalytic $H_2$ evolution experiments**

Dye-sensitized photocatalytic $H_2$ evolution experiments were performed with a PCX50C Discover multichannel photocatalytic reaction system (Beijing Perfectlight Technology Co. Ltd.) with white-light LED lamps (10 W×9, 380 nm≤λ≤780 nm, 100 mW $cm^2$) as the light source. In a typical procedure, ErB and $MoSi_2$ powders were added to a quartz reactor (60 mL) containing 25 mL of 10 vol.% TEOA aqueous solution under vigorous stirring. The pH values of the reaction solution were adjusted by addition of hydrochloric acid or sodium hydroxide. Then, the reaction solution was

thoroughly degassed by repeated evacuation and $N_2$ refilling processes, and finally refilled with $N_2$ to reach an ambient pressure. After that, the reaction solution was irradiated under continuous stirring. The amount of $H_2$ produced was manually taken out by a gas-tight syringe (Agilent, 1.0 mL) and analyzed at given time intervals with a calibrated gas chromatography (Tech comp; GC-7900) with a thermal conductivity detector, a 5 Å molecular sieve column (4 mm×5 m), and with $N_2$ as carrying gas.

To evaluate the photocatalytic $H_2$ evolution activities of CdS/$MoSi_2$ (10 wt%) and $TiO_2$/$MoSi_2$ (10 wt%) composite photocatalysts, the $H_2$ evolution experiments were carried out in 250 mL reaction cell connected to a closed gas circulation and evacuation system (CEL-SPH2N, CEAULIGHT). A 300-W Xe lamp (CEL-HXF300) was used as light source (320 nm≤$\lambda$≤800 nm), where a 420 nm cut-off filter was equipped when CdS/$MoSi_2$ (10 wt%) was used as the photocatalyst. Typically, 50 mg of photocatalyst was dispersed in 100 mL of TEOA (10 vol%, pH 10) solution by ultrasonication for 10 min. Before light irradiation, the reaction system was thoroughly degassed by evacuation in order to remove the oxygen inside the reactor and dissolved in solution. The reaction solution was continuously stirred and maintained at 6 °C by a flow of cooling anhydrous ethanol.

**1.5 Electrochemical measurements**

The electrochemical measurements were carried out in a standard three-electrode electrochemical set-up using a CS3103 (Wuhan Corrtest Instruments Corp., Ltd) electrochemical workstation. The saturated Ag/AgCl and graphite rod were used as reference electrode and counter electrode, respectively. For the fabrication of working electrode, the catalyst suspension was prepared by dispersing 20 mg of $MoSi_2$ powder into 1 mL of ethanol/$H_2O$ (4/1, v/v) mixed solution containing 100 μL of 0.5 wt% Nafion solution by ultrasonication for 15 min. Afterward, the as-prepared catalyst suspension was loaded onto carbon paper (HESEN, HCP030P, thickness, 0.3 mm). The loading amount of $MoSi_2$ on carbon paper was controlled to be 0.8 mg $cm^{-2}$. The electrocatalytic activity of $MoSi_2$ towards $H_2$ evolution was examined by obtaining polarization curves using linear sweep voltammetry (LSV) at a scan rate of 5 mV $s^{-1}$ in

a 0.5 M $Na_2SO_4$ solution containing TEOA (10 vol%, pH 10). All the applied potentials are reported as reversible hydrogen electrode potential scale using $E$ (vs. RHE)=$E$ (vs. Ag/AgCl)+0.2142 V after $IR_s$ correction. Potentiostatic electrochemical impedance spectroscopy (EIS) was used to determine the uncompensated solution resistance ($R_s$). EIS measurements were carried out at an AC amplitude of 5 mV in the frequency range of 10 mHz to 100 kHz.

**1.6 DFT calculations**

The Perdew-Burke-Ernzerhof (PBE) functional in the Vienna Ab initio Simulation Package (VASP) was adopted in all calculations, and the weak interaction was considered using the DFT-D3 van der Waals correction. In the calculation, the plane-wave cutoff energy of 450 eV and the vacuum space of 15 Å were employed. The Brillouin-zone was meshed by a γ-centered 2×4×1 $k$-points grid. The geometry of $MoSi_2$ (103) included 52 Si and 28 Mo atoms. The energy difference smaller than $1\times10^{-6}$ eV and the force of each atom less than 0.01 eV $Å^{-1}$ were chosen as the convergence criterion of geometry optimization. In the calculations, all atoms were allowed to relax. The free energy of the adsorbed H ($\Delta G_H$) was calculated by $\Delta G_H = \Delta E_H + \Delta E_{ZPE} - T\Delta S$ (eV), where $\Delta E_{ZPE}$ and $\Delta S$ were the changes in the zero-point energy and entropy between H adsorption and $H_2$ in the gas phase, respectively. The $\Delta E_H$ were computed using $\Delta E_H\,(\mathrm{eV}) = E_{M\text{-}H} - E_M - \frac{1}{2}E_{H_2}$.

## 2. Supplementary data

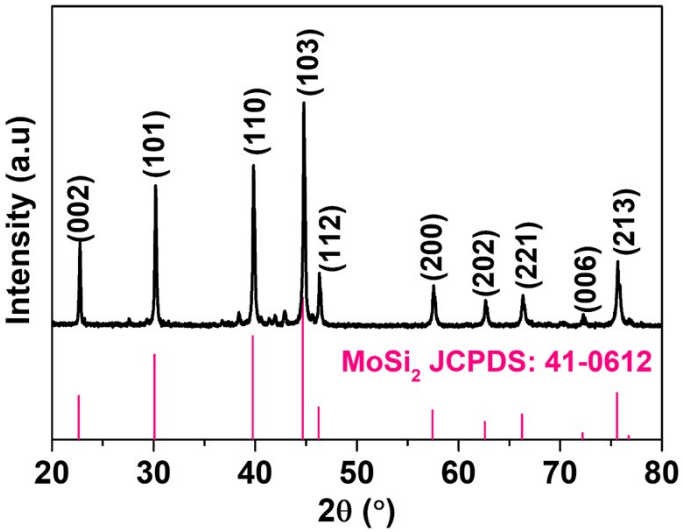


**Fig.S1** XRD pattern of as-received $MoSi_2$ powder.

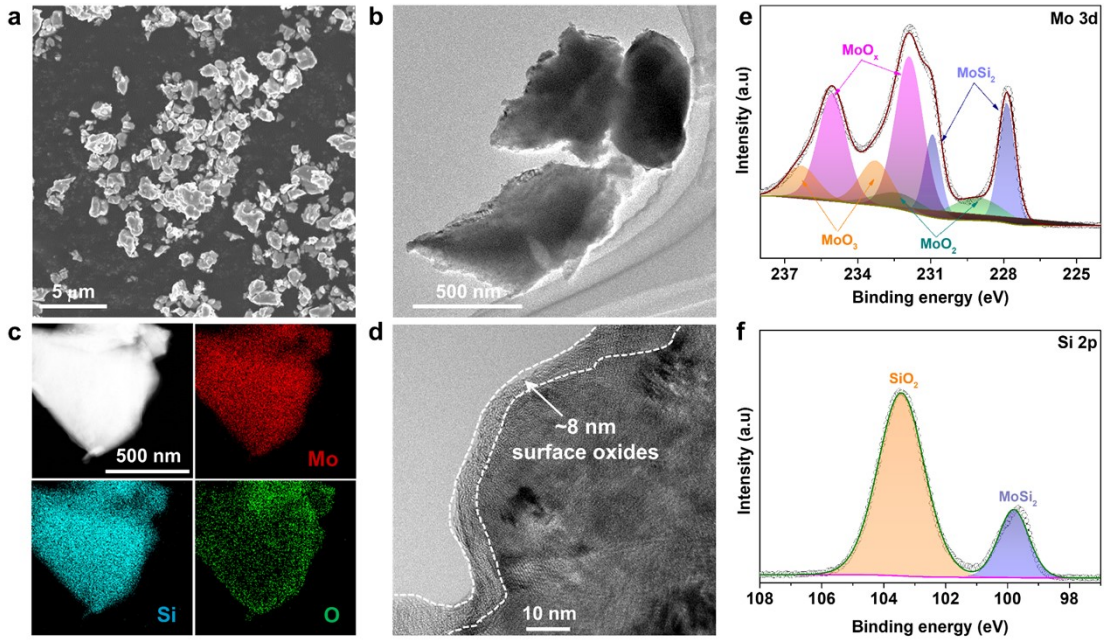


**Fig. S2** (a) SEM, (b) TEM, (c) HAADF-STEM and the corresponding EDX, and (d) HRTEM images of as-received $MoSi_2$ powder. (e) Mo 3d and (f) Si 2p XPS spectra of as-received $MoSi_2$ powder.

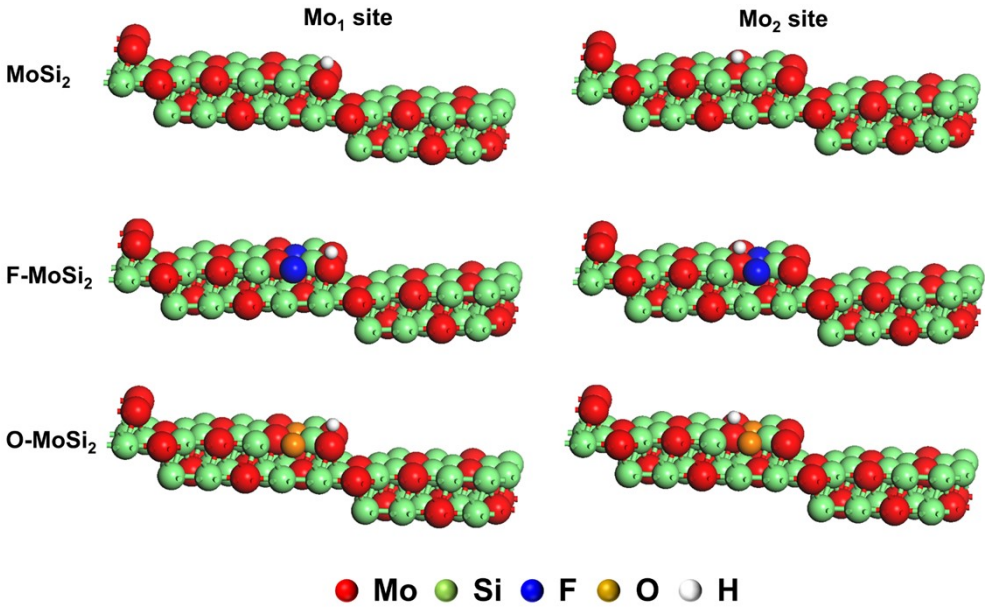


**Fig. S3** The side views of H adsorption at different Mo sites ($Mo_1$ and $Mo_2$) on the surface of 2×2×1 pure $MoSi_2$, O-doped $MoSi_2$ (O-$MoSi_2$), and F-doped $MoSi_2$ (F-$MoSi_2$) supercells.

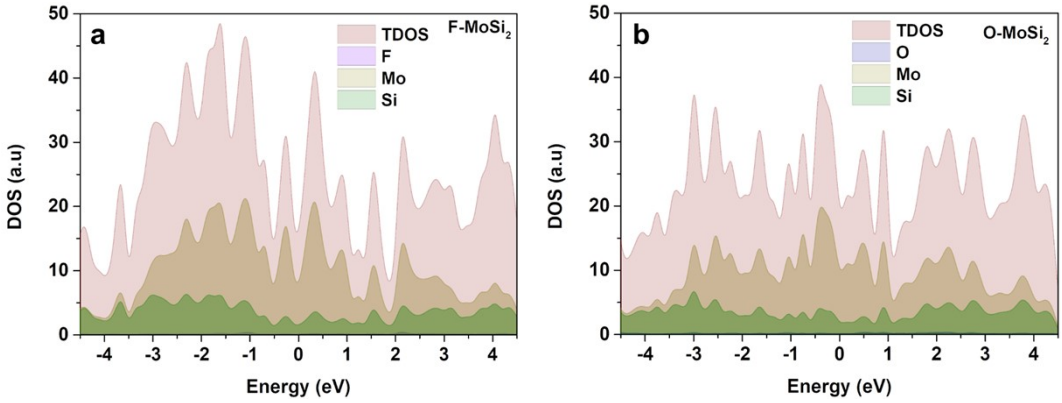


**Fig. S4** The total density of states (TDOS) and partial density of states for (a) F-$MoSi_2$ and (b) O-$MoSi_2$.

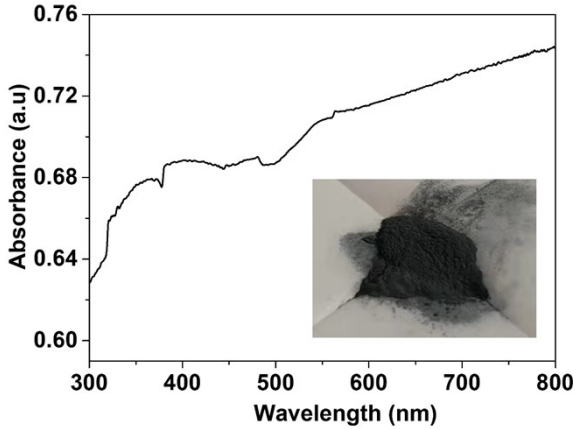


**Fig. S5** UV-vis absorption sepctrum of etched $MoSi_2$ powder. The inset is a photograph of the $MoSi_2$ powder.

**Table S1.** Electrocatalytic $H_2$ evolution performances of recently reported Mo-based and transition metal silicide catalysts.

| Catalyst | Electrolyte | Overpotential ($\eta_{10}$) at 10 mA $cm^{-2}$ (mV) | Tafel slope (mV $dec^{-1}$) | Ref. |
|---|---|---|---|---|
| $MoS_2$/RGO | 0.5 M $H_2SO_4$ | 150 | 41 | [S4] |
| $MoS_2$-GNR | 0.5M $H_2SO_4$ | 160 | 50 | [S5] |
| Amorphous $MoS_{2+x}$ | 0.5 M $H_2SO_4$ | 160 | 40 | [S6] |
| $MoS_2$/carbon | 0.5M $H_2SO_4$ | 103 | 56 | [S7] |
| $MoSe_2$ | 0.5 M $H_2SO_4$ | 107.2 | 31 | [S8] |
| MoP@NC | 1M KOH | 129.3 | 57.94 | [S9] |
| $Mo_2N$/NC | 0.5 M $H_2SO_4$ | 217 | 115.7 | [S10] |
| Defect-rich MoN | 0.5 M $H_2SO_4$<br>1 M KOH | 125<br>139 | 51.2<br>67.8 | [S11] |
| MoP-NC/MoP-C/CC | 0.5M $H_2SO_4$ | 74 | 59 | [S12] |
| MoP | 1 M KOH | 220 | 154 | [S13] |
| MoP@NC | 1 M KOH | 96 | 53 | [S13] |
| MoC@NC | 1M KOH | 160 | 55 | [S14] |
| Graphene/$Mo_2C$ | 0.5 M $H_2SO_4$ | 270 | 56 | [S15] |
| $Mo_2C$ | 0.5 M $H_2SO_4$<br>1 M KOH | 210<br>192 | 56<br>54 | [S16] |
| MoB | 0.5 M $H_2SO_4$<br>1 M KOH | 212<br>218 | 55<br>59 | [S16] |
| LaRuSi | 1 M KOH | 72 | 68 | [S17] |
| $Pd_2Si$ | 0.5 M $H_2SO_4$ | 192 | 131 | [S18] |
| $Ni_2Si$ | 0.5 M $H_2SO_4$ | 243 | 66 | [S18] |
| $Mo_5Si_3$ | 0.5 M $H_2SO_4$ | 80 | 65.1 | [S19] |
| $MoSi_2$ | 0.5 M $H_2SO_4$ | 94 | 71.2 | [S19] |
| $MoSi_2$ | 0.5 M $NaSO_4$/10 vol% TEOA (pH 10) | 138 | 117.2 | This work |

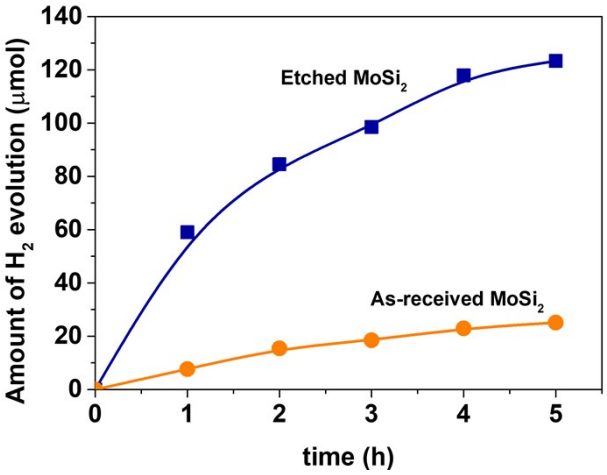


**Fig. S6** Time courses of $H_2$ evolution catalyzed by as-recieved and etched $MoSi_2$ from ErB-TEOA system. Light source: white LED lamp, 380 nm ≤$\lambda$≤780 nm; TEOA solution: 25 mL, 10 vol%, pH 10; catalyst: 5.0 mM.

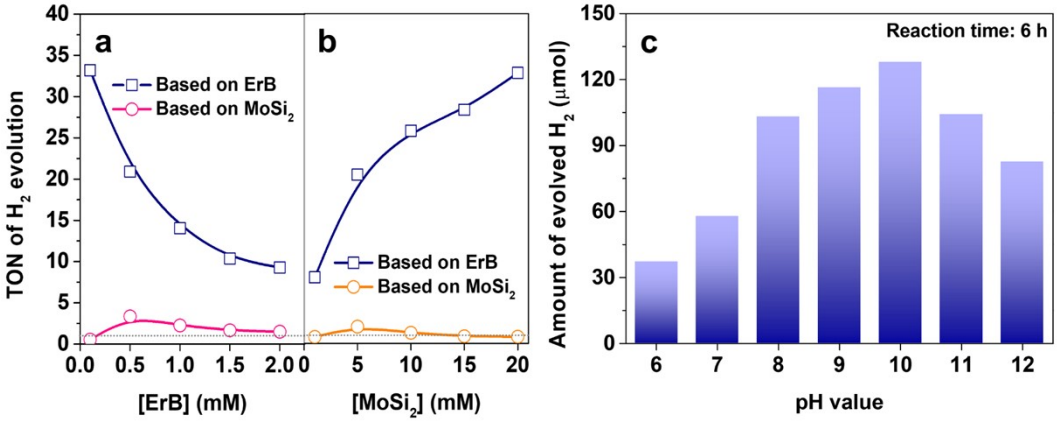


**Fig. S7** (a) TON of $H_2$ evolution from the systems containing 5 mM of $MoSi_2$ and different concertrations of ErB in a TEOA solution (pH 10). (b) TON of $H_2$ evolution from systems containing 0.5 Mm ErB and different concertrations of $MoSi_2$ in a TEOA solution (pH 10). (c) Effect of the pH value of TEOA solution on the photocatalytic $H_2$ evolution from the system containing ErB (0.5 mM) and $MoSi_2$ (5 mM). Other reaction conditions: Light source: white LED lamp, 380 nm ≤$\lambda$≤780 nm; TEOA solution: 25 mL, 10 vol%.

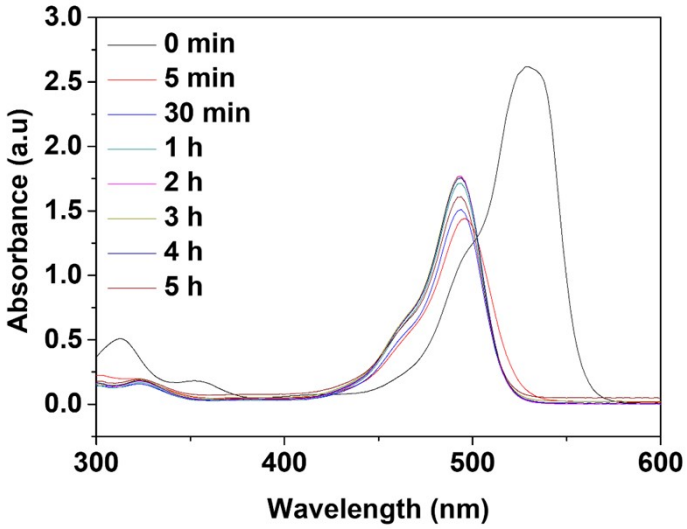


**Fig. S8** Time-depedent UV-vis absorption spectra of the system containing ErB (0.5 mM) and $MoSi_2$ (4.0 mM) in a TEOA solution (10 vol.%, 25 mL,) upon irradiation. The $MoSi_2$ particles were removed by centrifugation prior to measurement and the solution was diluted by 10 times. Reaction conditions: Light source: white LED lamp, 380 nm ≤$\lambda$≤780 nm; TEOA solution: 25 mL, 10 vol%, pH 10.

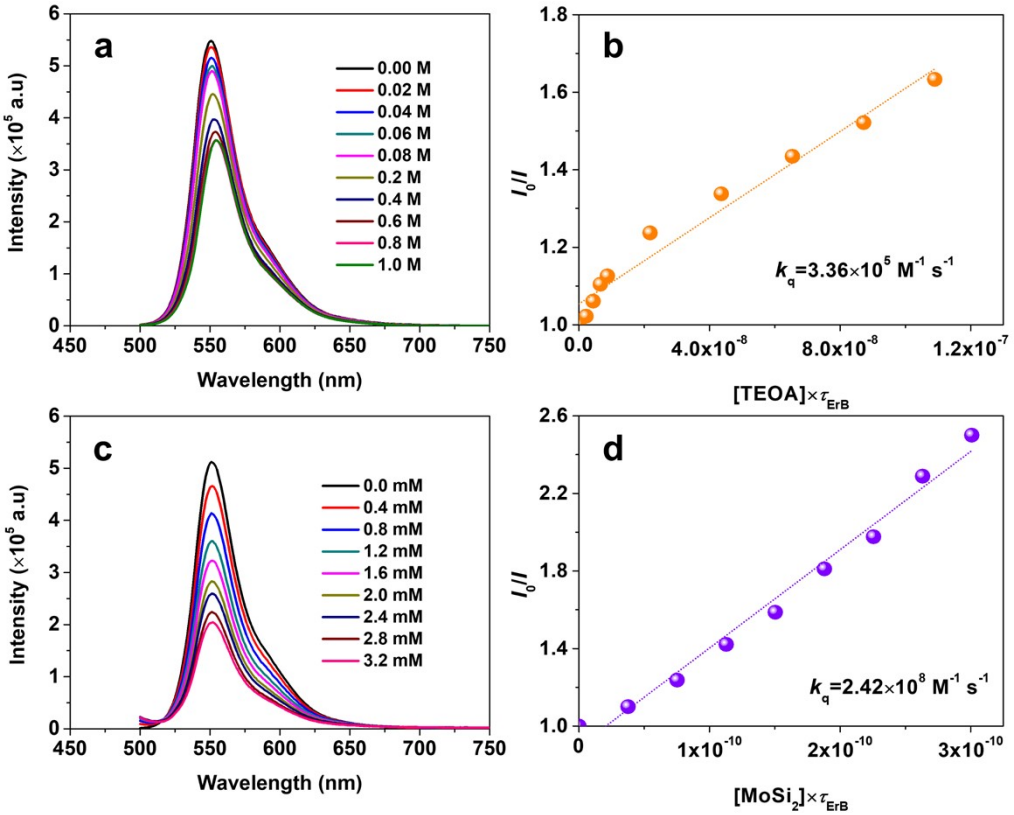


**Fig. S9** (a) PL mission quenching of ErB solution (10 mM) with TEOA and (b) the corresponding Stern–Volmer plot. (c) PL mission quenching of ErB solution (10 mM) with $MoSi_2$ and (d) the corresponding Stern-Volmer plot ($\tau_{ErB}$=0.15 ns).[S20]

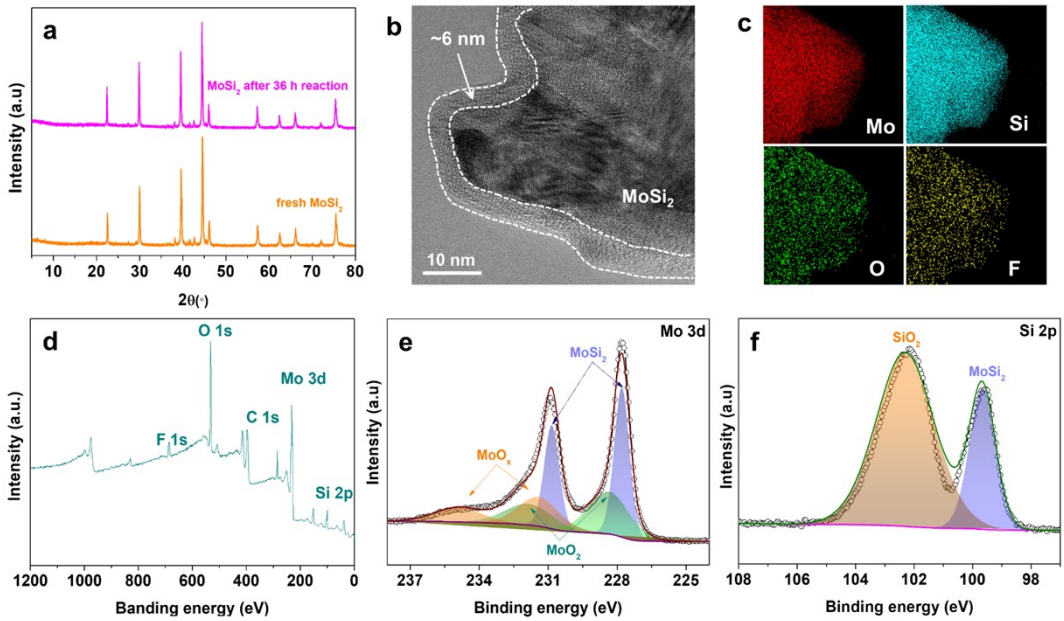


**Fig. S10** (a) A comparion for the XRD patterns of $MoSi_2$ before and after stability test. (b) HRTEM image and (c) EDX mapping images of $MoSi_2$ after stability test (d) XPS survey, (e) Mo 3d, and (f) Si 2p XPS spectra of $MoSi_2$ after stability test.

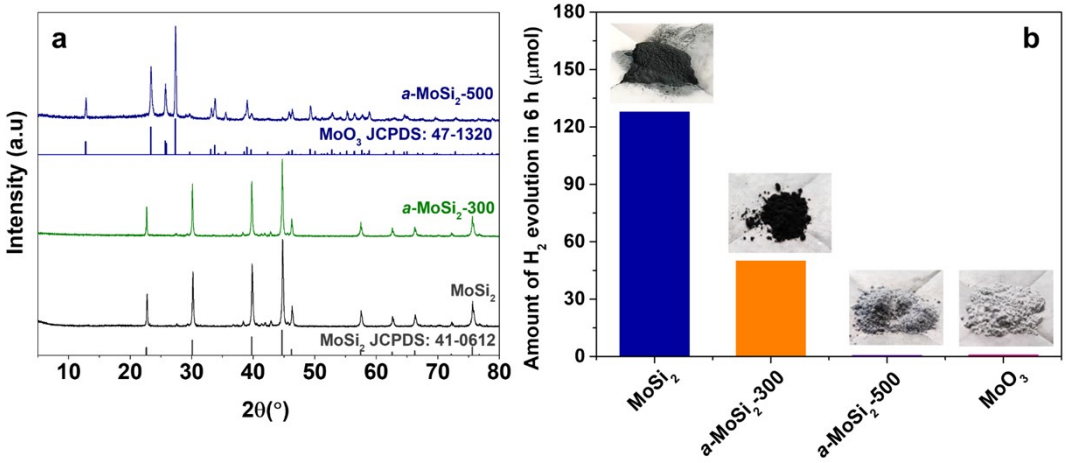


**Fig. S11** (a) XRD patterns of $MoSi_2$ and those air-annealed $MoSi_2$ at 300 (*a*-$MoS_{i2}$-300) and 500 °C (*a*-$MoS_{i2}$-300) for 2 h. (b) Catalytic $H_2$ evolution activity of air-annealed $MoSi_2$ from the system containing ErB in a TEOA solution. The air-annealing of $MoSi_2$ was carried out in air at different temperatures for 3 h, and the obtained samples were denoted as *a*-$MoSi_2$-*x*, where *x* represents the annealing temperature. Light source: white LED lamp, 380 nm ≤$\lambda$≤780 nm; TEOA solution: 25 mL, 10 vol%, pH 10. The insets in Figure S10b are the photos of the catalysts.

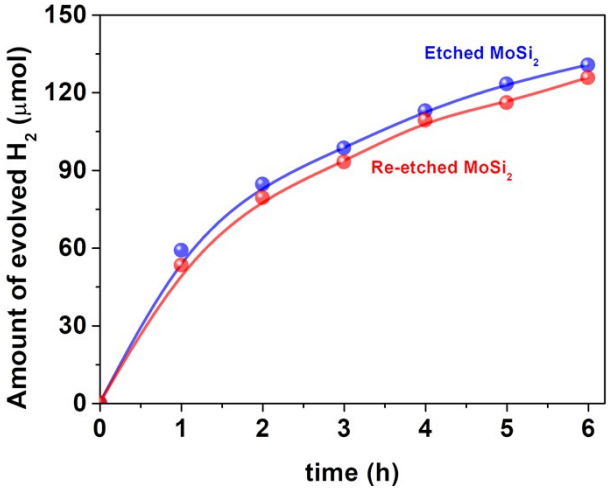


**Fig. S12** Catalytic $H_2$ evolution activities of etched $MoSi_2$ and the used $MoSi_2$ after being re-etched with HF (1 M, 6 h) (termed as Re-etched $MoSi_2$) from the TEOA solution containing ErB. Light source: white LED lamp, 380 nm ≤$\lambda$≤780 nm; ErB, 0.5 mM; catalyst: 5.0 mM; TEOA solution: 25 mL, 10 vol%, pH 10.

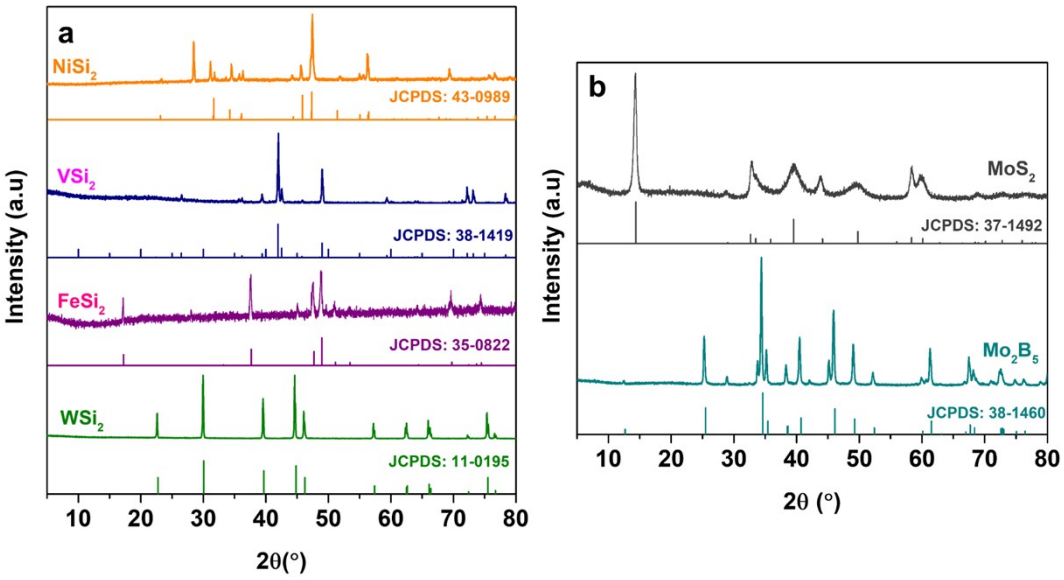


**Fig. S13** XRD patterns of other (a) transition metal disilicides including $WSi_2$, $FeSi_2$, $VSi_2$, and $NiSi_2$ and (b) Mo-based catalysts including $MoS_2$ and $Mo_2B_5$.

**Table S2** Specific surface areas of the catalysts

| Catalyst | $MoSi_2$ | $FeSi_2$ | $NiSi_2$ | $VSi_2$ | $WSi_2$ | $MoS_2$ | $Mo_2B_5$ |
|---|---|---|---|---|---|---|---|
| $S_{BET}$ ($m^2$ $g^{-1}$) | 5.8 | 2.9 | 1.7 | 2.4 | 3.6 | 2.3 | 3.5 |

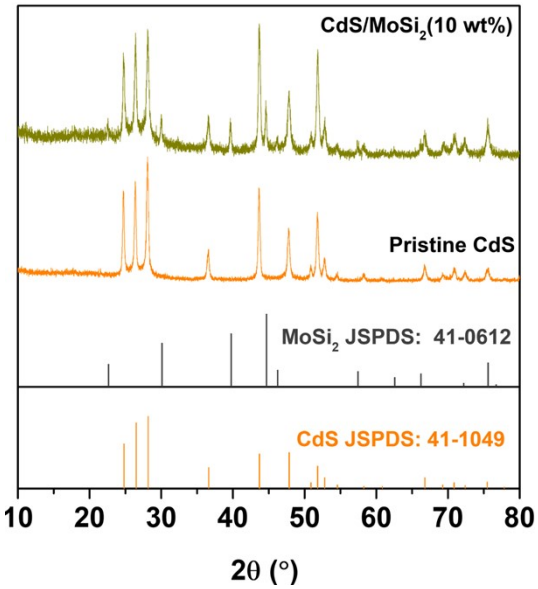


**Fig. S14** XRD patterns of CdS, $MoSi_2$, and CdS/$MoSi_2$ (10 wt%).

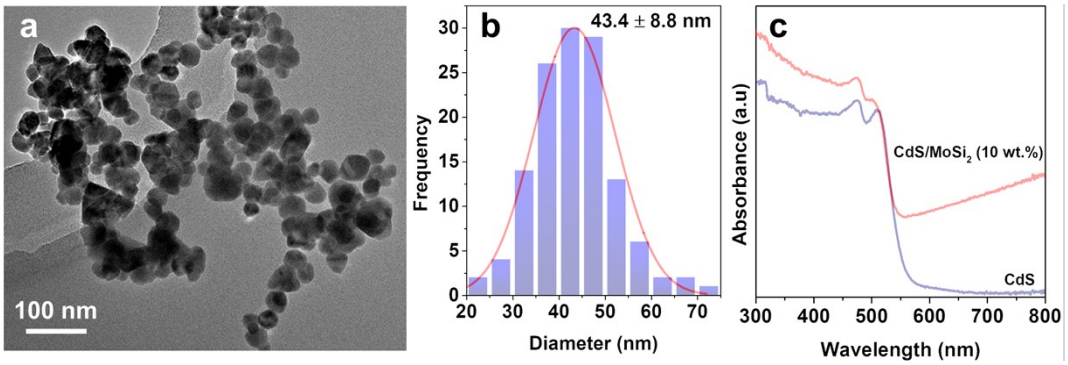


**Fig. S15** (a) TEM image and (b) the corresponding statistical diagram for particle size of pristine CdS. (c) UV-vis absorption spectra of pristine CdS and CdS/$MoSi_2$ (10 wt%).

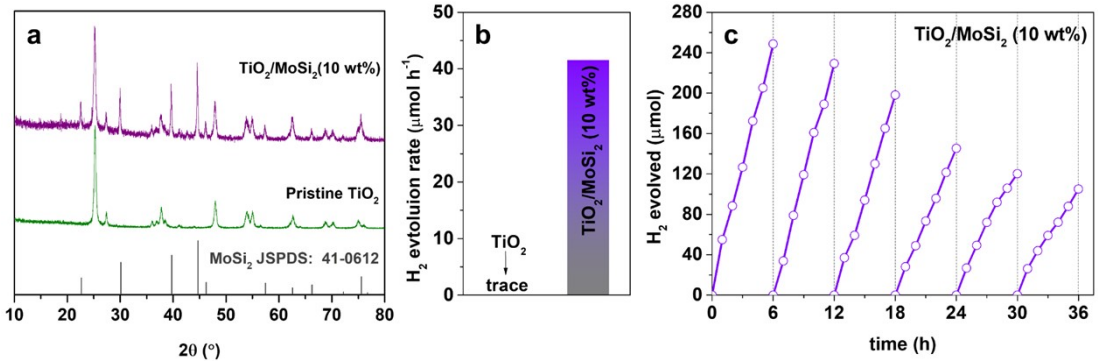


**Fig. S16** XRD patterns of $TiO_2$ and $TiO_2$/$MoSi_2$ (10 wt%). (b) A comparison of the photocatalytic $H_2$ evolution activities of pristine $TiO_2$ and $TiO_2$/$MoSi_2$ (10 wt%) in a TEOA solution (10 vol%, pH 10) under full-spectrum irradiation of a 300-W Xe lamp. (c) Cycling stability of $TiO_2$/$MoSi_2$ (10 wt%) toward photocatalytic $H_2$ evolution over a period of 36 h.

**Supplementary References**

[S1] X. Zong, Z. Xing, H. Yu, Y. Bai, G. Lu and L. Wang, *J. Catal*., 2014, **310**, 51.

[S2] L. Tian, S. X. Min and F. Wang, *Appl. Catal. B* 2019, **259,** 118029.

[S3] F. Wang, X. Liu, Z. Zhang and S. Min, *Chem. Commun.,* 2020, **56**, 3281.

[S4] Y. Li, H. Wang, L. Xie, Y. Liang, G. Hong and H. Dai, *J. Am. Chem. Soc.,* 2011, **133**, 7296.

[S5] J. Ekspong, R. Sandström, L. Rajukumar, M. Terrones, T. Wågberg and E. Gracia-Espino, *Adv. Funct. Mater.,* 2018, **28**, 1802744.

[S6] H. Vrubel and X. Hu, *ACS Catal.,* 2013, **3**, 2002.

[S7] L. Yang, W. Zhou, J. Lu, D. Hou, Y. Ke, G. Li, Z. Tang, X. Kang and S. Chen, *Nano Energy* 2016, **22**, 490.

[S8] D. Damien, A. Anil, D. Chatterjee and M. M. Shaijumon, *J. Mater. Chem. A* 2017, **5**, 13364.

[S9] P. Wei, X. Li, Z. He, Z. Li, X. Zhang, X. Sun, Q. Li, H. Yang, J. Han and Y. Huang, *Appl. Catal. B* 2021, **299**, 120657.

[S10] Y. Song and Z. Yuan, *Electrochim. Acta* 2017, **246,** 536.

[S11] J. Xiong, W. Cai, W. Shi, X. Zhang, J. Li, Z. Yang, L. Feng and H. Cheng, *J. Mater. Chem. A* 2017, **5**, 24193.

[S12] B. Liu, H. Li, B. Cao, J. Jiang, R. Gao and J. Zhang, *Adv. Funct. Mater.,* 2018, **28**, 1801527.

[S13] J. Li, H. Huang, X. Cao, H. Wu, K. Pan, Q. Zhang, N. Wu and X. Liu, *Chem. Eng. J.,* 2021, **416**, 127677.

[S14] X. Zhou, Y. Tian, J. Luo, B. Jin, Z. Wu, X. Ning, L. Zhan, X. Fan, T. Zhou, S. Zhang and X. Zhou, *Adv. Funct. Mater.*, 2022, **32**, 2201518.

[S15] S. Chaitoglou, T. Giannakopoulou, G. Papanastasiou, D. Tsoutsou, A. Vavouliotis, C. Trapalis and A. Dimoulas, *Appl. Surf. Sci.,* 2020, **510**, 145516.

[S16] H. Vrubel and X. Hu, *Angew. Chem. Int. Ed.,* 2012, **51**, 12703.

[S17] S. Shen, Z. Hu, H. Zhang, K. Song, Z. Wang, Z. Lin, Q. Zhang, L. Gu and W. Zhong, *Angew. Chem. Int. Ed.* 2022, **61**, e202206460.

[S18] J. M. McEnaney and R. E. SchaakY. *Inorg. Chem.,* 2015, **54**, 707.

[S19] Y. Su Y. Xie, H. Qin, Z. Huang, Q. Yin, Z. Li, R. Zhang, Z. Zhao, F. Wu and G. Ou, *Int. J. Hydrogen Energy* 2022, **47**, 28924.

[S20] S. Li, H. Y. Zhang, R. Lu and A. C. Yu, *Spectroc Acta Pt. A-Molec. Biomolec. Spectr.,* 2017, **184**, 204.